The Advance towards WANDA Multi-phase: Simulations of Fast Transients in Multi-phase Pipelines

AGTJ Heinsbroek, Ph.D., M.Sc., H Hartmann, Ph.D., M.Sc.
Deltares | Delft Hydraulics, Delft, The Netherlands

ABSTRACT

This paper presents results of gas dynamics simulations in a multi-phase (gas/condensate) pipeline. The code is already applied in various consultancy projects concerning choke-valve break-out and it is part of the ongoing development of a gas dynamics module that will be integrated within the (currently single-phase) WANDA© software package.

The choke-valve break-out scenario has been simulated with our newly developed validated code which solves for transient flow of compressible fluids through pipelines by solving the conservation laws of mass, momentum and energy combined with a constitutive law (ideal gas law and others). In this way, the model is able to solve for pressure surges with a variable, temperature dependent wave speed. Furthermore, the model accounts for the presence of liquid slugs in local depressions of the pipeline, which will even further force up pressure due to reflection of the travelling pressure wave.

NOMENCLATURE

A	Cross sectional area	[m^2]	P	Pressure	[Pa]
A_v	Discharge coeff. (=$2.4\cdot10^{-5}C_v$)	[m^2]	R	Gas constant	[J/kg·K]
C	Pressure wave speed	[m/s]	T	Temperature	[K]
C_T	Isothermal pressure wave speed	[m/s]	t	Time	[s]
C_v	Discharge coefficient	[GPM/√psi]			
c_p	Specific heat	[J/kg·K]	V	Velocity	[m/s]
c_v	Specific heat	[J/kg·K]	W	Mass flow	[kg/s]
D	Pipe internal diameter	[m]	X	Pressure ratio valve $(P_1\text{-}P_2)/P_1$	[–]
F_k	Ratio of k with k_{air} (= k/1.4)	[–]	x	Coordinate along pipe	[m]
F_{fr}	Wall pressure force (axial)	[N/m^2]	Y	Gas expansion factor of valve	[–]
f	Friction coefficient	[–]	Z	Compressibility factor	[–]
g	Gravitational acceleration	[m/s^2]	ϕ	Heat flow	[W]
k	Ratio of specific heats (c_p/c_v)	[–]	ρ	Density	[kg/m^3]
L	Length	[m]	τ_w	Shear stress	[Pa]

1 INTRODUCTION

In the computation of fast transients in gas pipeline systems it is essential to take into account the full thermodynamic behaviour of the gas and the boundary conditions. Examples of such fast transient phenomena are choke valve break-out with or without the effects of initial slugs, full blow out of gas wells, severe slugging problems and long slugging problems. Also the accurate computation of the rarefaction waves in the gas well in the first two examples requires full thermodynamic modelling.

Currently, there is a trend of developing more and more mechanistic models to simulate the dynamic behaviour of pipeline flow in order to to decrease the dependency on empirical correlations. This is expected to improve the predictive power of the simulations. The model in this paper is a first step in the development towards unsteady multi-phase flow analysis over the full spectrum of void fractions.

The application range of the Deltares|Delft Hydraulics fluid dynamics (waterhammer) computer code WANDA is steadily expanded. Already since many years the code contains multiphase effects, such as cavitation, column separation, free surface flow for priming and draining pipes, as well as air valve and air vessel components. These capabilities are used to simulate accurately – on a relatively small time scale – the fast transient phenomena arising from closing valves, tripping pumps with and without closing checkvalves, and closing of air valves and column separation cavities. The current extension towards highly transient gas dynamics fits very well in the mechanistic type of analyses carried out with WANDA. The gas dynamics extension concerns the pipe as well as the valve and compressor models.

In the subsequent sections the mathematical model of pipe and valve, an example of validation with measured data and a case study of a choke valve break-out transient are described. In the last section some conclusions are given.

2 MATHEMATICAL MODEL

At present the WANDA gas flow model is capable of describing a serial pipeline system including valves, diameter changes and boundary conditions. In the near future this will be generalised to branched and looped pipeline networks. Conservation models for mass, momentum and energy are applied and these will be elaborated in the following sections.

2.1 Pipeline model

The standard one-dimensional conservation equations are used:

Mass conservation:

$$\left(\frac{\partial \rho}{\partial t} + V\frac{\partial \rho}{\partial x}\right) + \rho\frac{\partial V}{\partial x} = 0 \tag{1}$$

Momentum conservation:

$$\rho\left(\frac{\partial V}{\partial t} + V\frac{\partial V}{\partial x}\right) + \frac{\partial P}{\partial x} = -\frac{4\tau_w}{D} - \rho g \sin\theta \tag{2}$$

Energy conservation:

$$\rho c_{\mathrm{p}}\left(\frac{\partial T}{\partial t}+V\frac{\partial T}{\partial x}\right)=\left(\frac{\partial P}{\partial t}+V\frac{\partial P}{\partial x}\right)+\frac{4\tau_{\mathrm{w}}V}{D}+\frac{\phi}{A} \tag{3}$$

To close the relation between the four unknowns P, V, T and ρ, the simple equation of state of an ideal gas with (assumed constant) compressibility factor is used:

$$P = Z R \rho T \tag{4}$$

More advanced gas models can be easily implemented in the code later on.

Considering the theory of thermodynamics, the continuity equation (1) can be rewritten in the following format:

$$\frac{1}{C^2}\left(\frac{\partial P}{\partial t}+V\frac{\partial P}{\partial x}\right)+\rho\frac{\partial V}{\partial x}=\frac{1}{c_{\mathrm{p}}T}\left(\frac{4\tau_{\mathrm{w}}V}{D}+\frac{\phi}{A}\right) \tag{5}$$

The transient pressure waves are fast enough to assume an adiabatic process. Therefore the wave speed C is considered isentropic and temperature dependent:

$$C = \sqrt{ZkRT} \tag{6}$$

The right hand side term in equation (5) accounts for the thermal expansion of the gas due to frictional heat generation and heat exchange through the pipe wall. This equation is a generic equation taking into account the full gas thermodynamics.

When assuming isothermal gas flow, in equation (3) the total derivative of the temperature becomes zero:

$$-\left(\frac{\partial P}{\partial t}+V\frac{\partial P}{\partial x}\right)=\frac{4\tau_{\mathrm{w}}V}{D}+\frac{\phi}{A} \tag{7}$$

Inserting this in equation (5) leads to:

$$\left(\frac{1}{C^2}+\frac{1}{c_{\mathrm{p}}T}\right)\left(\frac{\partial P}{\partial t}+V\frac{\partial P}{\partial x}\right)+\rho\frac{\partial V}{\partial x}=0 \tag{8}$$

Equation (8) reduces to:

$$\frac{1}{C_{\mathrm{T}}{}^2}\left(\frac{\partial P}{\partial t}+V\frac{\partial P}{\partial x}\right)+\rho\frac{\partial V}{\partial x}=0 \tag{9}$$

with the isothermal wave speed:

$$C_{\mathrm{T}} = \sqrt{Z R T} = \sqrt{P/\rho} \tag{10}$$

Equation (7) resembles the reasoning for isothermal gas flow as presented by Streeter and Wylie. In case of air considered to be an ideal gas, the isothermal pressure wave speed C_T differs from the adiabatic wave speed C by 20%. This deviation is not negligible in case of fast transient phenomena. Furthermore, fast transients often imply velocities comparable to the wave speed (e.g. the choke-valve break-out scenario presented in section 4), and consequently the convective terms cannot be neglected.

Wall friction is modelled according to White-Colebrook:

$$\tau_w = f \frac{\rho}{8} V |V| \tag{11}$$

In each point of the internal computational grid the three state variables P, V and T and are solved simultaneously (using ρ of the previous timestep) by transforming the equations (2), (3) and (5) according to the method of characteristics into pressure/velocity relations and energy flux relations. Finally, the density ρ at the new timestep is calculated using the equation of state (4). Since the characteristic directions $C+V$ and $C-V$ vary with the varying wave speed and flow velocity, the starting points of the characteristics have to be interpolated between the grid points. The interpolation points are determined such that the characteristics exactly intersect at the grid points for the new time steps. More advanced (curved) characteristics may be employed, but have not yet been implemented in the current computational model.

2.2 Diameter change model

This is in fact a generalisation of an internal computational point within a pipe. The state variables are split at both sides of the junction, yielding eight unknowns to be solved: P_1, V_1, T_1, ρ_1, P_2, V_2, T_2, and ρ_2. Three of the needed eight equations are delivered by the characteristic equations of the adjacent pipes (two pressure-velocity characteristics and one energy flux characteristic of the pipe with its mass flow towards the connecting node). The two endpoints of the pipes each deliver one equation of state (4). The remaining three equations are resulting from conservation of mass, momentum and energy over the node:

Mass conservation:

$$\rho_1 V_1 A_1 - \rho_2 V_2 A_2 = 0 \tag{12}$$

Momentum conservation:

$$\left(P_1 + \rho_1 V_1^2\right) A_1 - \left(P_2 + \rho_2 V_2^2\right) A_2 = F_{fr} \tag{13}$$

Energy conservation:

$$\left(c_p T_1 + \frac{V_1^2}{2}\right) - \left(c_p T_2 + \frac{V_2^2}{2}\right) = 0 \tag{14}$$

The flow through the node is assumed to be lossless and adiabatic.

2.3 Valve model

A valve is located between two pipes of equal cross sectional area. Like with the diameter change model, we have eight state variables to be solved. The adjacent pipes and connection points again deliver five of the equations. The first of the remaining three equations are the simplified mass conservation equation ($A_1 = A_2$):

$$\rho_1 V_1 - \rho_2 V_2 = 0 \tag{15}$$

For the second equation a much used empirical compressible flow relation of the valve is applied:

$$W\left(=\rho_1 A_1 V_1\right) = A_v Y \sqrt{X P_1 \rho_1} \tag{16}$$

The gas expansion factor Y changes with the pressure ratio X and is truncated when critical (choking) flow occurs in the valve,

$$Y = 1 - \frac{\min(X, X_T)}{3F_k X_T}, \qquad X = \frac{P_1 - P_2}{P_1} \tag{17), (18}$$

For the last equation again energy conservation is assumed (9). In reality, the relation between upstream and downstream temperature may be more complicated.

2.4 Boundary conditions

Two types of boundary conditions have been modelled: 1) the reservoir and 2) the closed end.

2.4.1 Reservoir

The down-hole reservoir boundary is simplified to a description of pressure and temperature as functions of time. Together with the pressure/velocity characteristic of the adjacent pipe element and the equation of state, the four state variables can be solved.

2.4.2 Closed end

The closed end of a pipe is modelled by the prescription of zero velocity and the energy equation (3) adapted to zero flow:

$$V = 0 \tag{19}$$

$$\rho c_p \frac{dT}{dt} - \frac{dP}{dt} = 0 \tag{20}$$

Together with the pressure/velocity characteristic of the adjacent pipe element and the equation of state, the four state variables can be solved.

2.5 Slug model

For choke valve break out during start-up the slugs are assumed to consist of liquid columns, which have collected at local depressions in the pipeline profile, taking into account the distribution of the hold-up. As a worst case calculation (to maximise the pressure reflections of the gas) these liquid columns will be accelerated in their entirety by the pressure differences over the column length (the so called rigid column theory). The velocities at both sides (and within) the liquid column do not vary with distance, only with time:

$$V_1 - V_2 = 0 \tag{21}$$

The acceleration of the slug is modelled as:

$$P_1 - P_2 - \rho_{slug} L_{slug} \frac{dV_1}{dt} - \frac{f_{slug} L_{slug}}{D} \rho_{slug} \frac{V_1 |V_1|}{2} = 0 \tag{22}$$

The temperature upstream of the slug is computed by the energy characteristic of the connected pipe. The temperature downstream is calculated by adiabatic expansion or compression described by:

$$\rho_2 c_p \frac{dT_2}{dt} - \frac{dP}{dt} = 0 \tag{23}$$

3 VALIDATION SHOCK-TUBE EXPERIMENT

In this section we present a validation experiment of the gas model as presented in section 2. A typical example of a benchmark experiment focusing on a fast transient phenomenon is the shock-tube experiment reported by Huber et al (1949). The geometry of the test section is shown in Figure 3.1. High and low pressure chambers filled with air are initially separated by a diaphragm. The pressure ratio equals 2.0. At t = 0, the diaphragm ruptures which initiates a travelling shockwave.

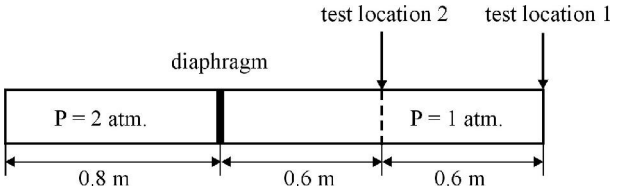

Figure 3.1. Shock-tube geometry.

A comparison between the measured and calculated pressure at two locations is shown in Figure 3.2. After rupture of the diaphragm a compression wave of magnitude 0.4 bar travels to the right passing location 2 after 1.5 ms. The wave arrives at location 1 at 3.0 ms and is reflected at the closed end. The reflection factor is about 1.25, resulting in a reflected compression of 0.5 bar, resulting in a total pressure increase of 0.9 bar. The reflected wave returns at location 2 at 4.9 ms (4.5 ms in the experiment).

It can be concluded that the code is able to compute the expansion and compression phenomena inside an ideal gas accurately.

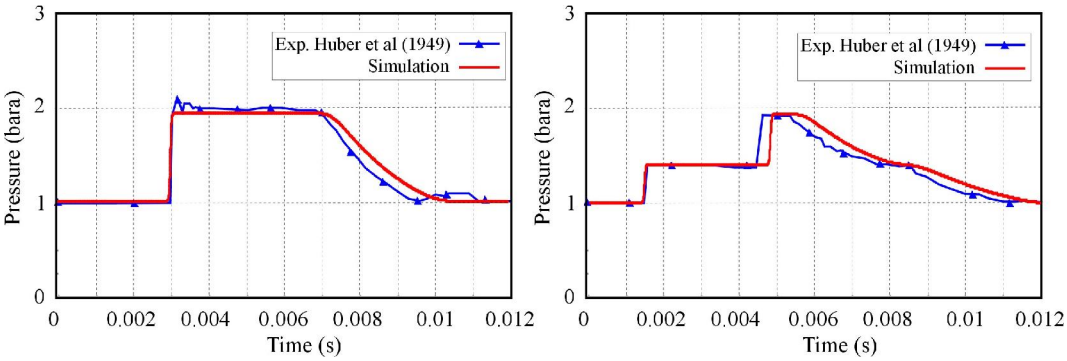

Figure 3.2. Pressure-time history at test location 1 (left) and test location 2 (right).

Note: Since the tube diameters left and right of the diaphragm are the same, the results are diameter independent.

4 APPLICATION CHOKE VALVE BREAK-OUT

In this section we focus on the choke valve break-out scenario. This scenario has been simulated in various consultancy projects and the relevance of this scenario is described in the following section.

4.1 Introduction

To reduce the FTHP (Flowing Tube Head Pressure) of a gas well to the operational pressure of the transport line a choke valve is generally applied. A High Integrity Pressure Protection System (HIPPS) serves to protect the downstream transport line against unacceptably high pressures in the case of choke valve failure. The HIPPS consists of two remotely operated valves (ROV) which are activated in case of an overpressure situation. In order to prevent the pressure in the transport line from exceeding the MAIP (Maximum Allowable Incidental Pressure), the HIPPS valves will close within 2 seconds after exceeding their set-pressure.

It is important to judge the performance of the HIPPS concept during an emergency condition, which can be a failure of the choke valve. This situation may occur in particular when upon start-up of a gas well hydrate plugs are propelled against the tungsten carbide trim cage of the choke valve. Due to the brittle nature of the material, the cage may completely break-out. The Cv-value of the choke valve will suddenly increase significantly, and a pressure wave will travel into the downstream system. Consequently, the HIPPS valves will close when the set-pressure is exceeded. A problem can occur when the HIPPS is not fast enough to be closed before the pressure in the transport line exceeds the MAIP.

The pressure in the transport line can be even further increased due to the presence of condensate slugs which have accumulated in the low sections of the transport line during the system standstill period. The effect of the presence of the slugs on the pressure on the transport line has been incorporated in our computer code (see section 2.5).

4.2 The system

A schematic picture of the system described in the previous section is shown in Figure 4.1. In the particular system shown in this figure, the presence of slugs in the first four low sections of the transport line is incorporated in the simulation model.

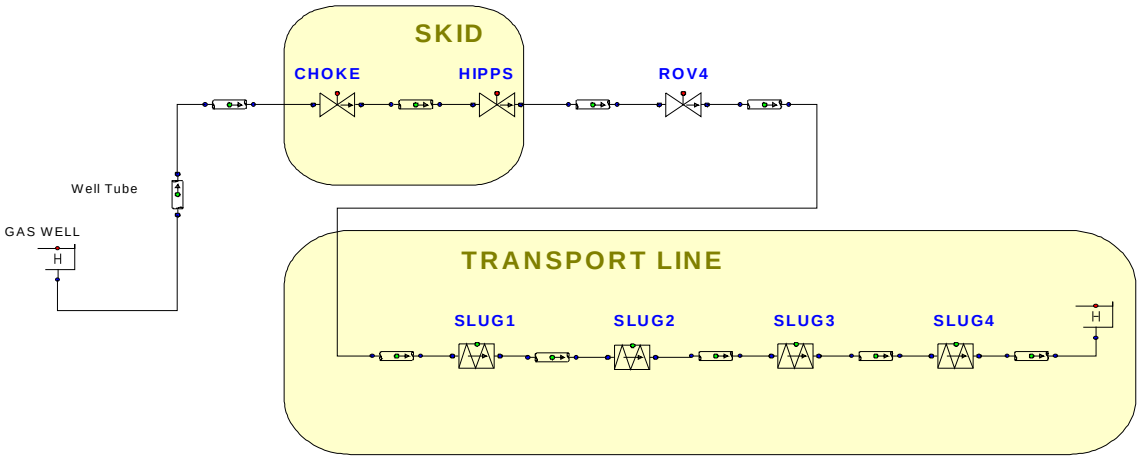

Figure 4.1. Schematic illustration of the system. The presence of slugs in the first four low sections of the transport line is incorporated in the simulation model.

Some relevant parameters of the modelled system are provided in **Table 4.1**.

Table 4.1 Some properties of the modelled system

GAS WELL	
Pressure gas well	272.5 bara
CITHP (Closed-In Tube Head Pressure)	221 bara
TRANSPORT LINE	
Initial pressure downstream choke valve	111 bara
Design pressure transport line	126 bara
Size transport line	6”
Length between entrance transport line and first depression in pipe profile	60 m
Length first depression	160 m
HIPPS VALVES	
Set-pressure	126 bara
Dead time	0.7 s
Closure time (100% - 0%)	1.3 s

4.3 Sensitivity analysis slug length

The slug length is usually computed by assuming that the full condensate hold-up accumulates at the lowest point in each depression of the pipe profile. If hold-up data have not been made available by the client, we follow an alternative conservative approach. This approach consists of a sensitivity analysis of the length of the first slug, since the inertia of the first slug is dominating the additional pressure rise in the transport line (the influence of the slugs further downstream is lower). The result of the sensitivity analysis will be further elaborated in detail below.

Time histories of the pressure at the entrance of the transport line are shown in Figure 4.2. The length of the first slug has been varied between 0 m and 160 m (i.e. the full length of the first depression). Directly after system start-up and failure of the choke valve the pressure rises from its initial level of 111 bara as a result of the passing pressure wave. The pressure wave reflects on the first slug and the influence of the inertia of this slug becomes clear from 0.4 seconds. The figure shows that increasing slug length leads to stronger pressure reflections, as expected. Furthermore, even in the most conservative situation of a maximum slug length of 160 m, the MAIP is not reached.

Figure 4.2 further indicates the closing procedure of the HIPPS valves. The set-pressure of these valves is exceeded from 0.35 seconds. The HIPPS valves start closing 0.7 seconds later (1.05 seconds after break-out) and are fully closed at 2.35 seconds. The maximum pressure in the transport line is reached in the dead time period of the HIPPS valves (0.35 – 1.05 seconds).

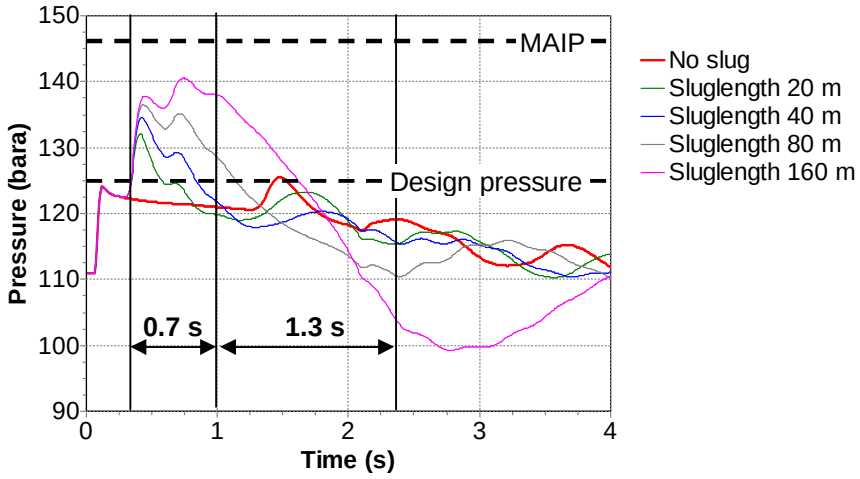

Figure 4.2 Pressure-time history at the entrance of the transport line. The length of the first slug varies between 0 m and 160 m. The HIPPS valves start closing from 1.05 s and are fully closed from 2.35 s.

4.4 Influence of mesh refinement

Subsequently to the sensitivity analysis we have studied the influence of the element length on the simulation results. The time history of the pressure at the entrance of the transport line is shown in Figure 4.3 for three different element lengths. The length of the first slug is 160 m. The figure shows that the element length does not have an effect of the main transient phenomena. The element length does affect the steepness of the travelling pressure wave, and the pressure reflections show more pronouncedly overshoots and undershoots. The results become grid independent at an element length of 1 m. To describe the length details of all pipe sections in the current case 15 m is the maximum element length possible. For practical considerations (representation of the different pipe lengths in the system) and high numerical resolution an element length of 1 m seems to be optimal.

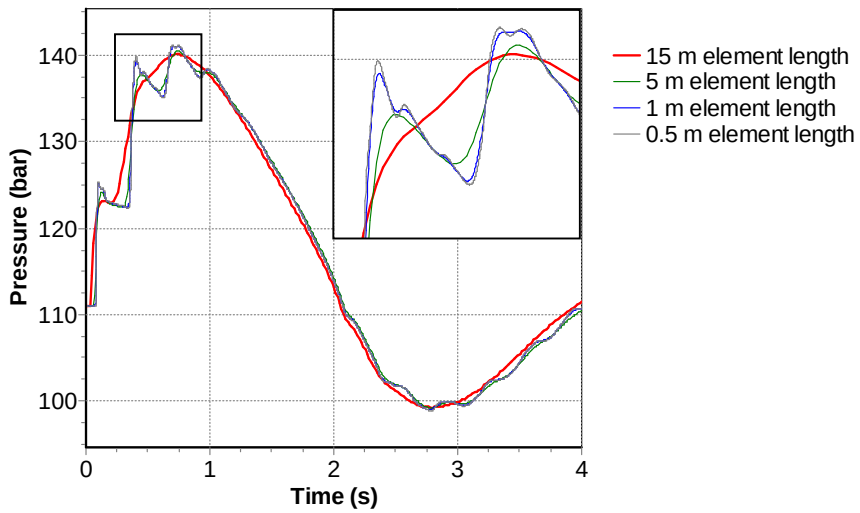

Figure 4.3 Influence of element length on pressure transient.

4.5 Spatial profiles

The pressure envelope (minimum and maximum pressures) and spatial pressure profiles at various instants in time are shown in Figure 4.4 for the complete system. This figure shows an overpressure wave propagating in the transport line and an underpressure wave into the well tube towards the gas well.

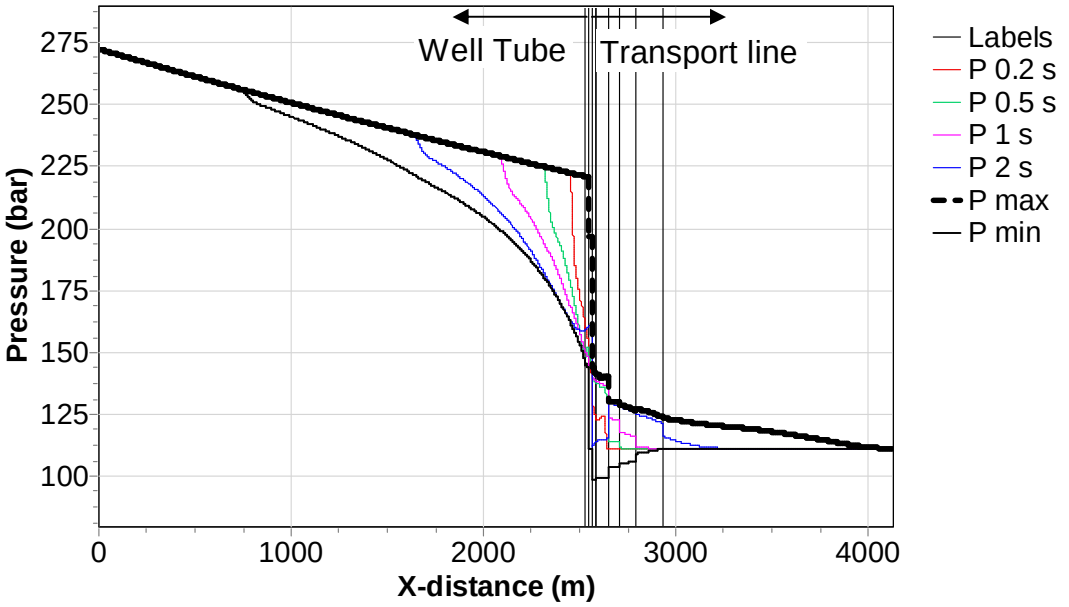

Figure 4.4 Pressure envelope (minimum and maximum pressures) and profiles at various time instants from gas well up to first part of the transport line.

Figure 4.5 shows the spatial pressure profiles in the first part of the transport line up to the location of the first slug. The pressure wave is reflected on this slug from t = 0.2 s. From this point in time, the slug accelerates up to a maximum velocity of 18.4 m/s (see Figure 4.6). Due to this increase in velocity, the pressure at the tail of the slug will decrease (compare pressure profiles at t = 0.25 s and t = 0.35 s at location X = 60 m).

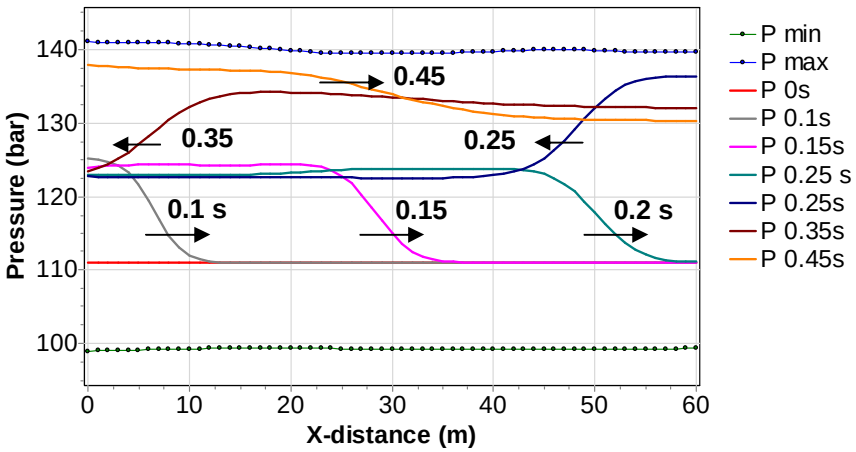

Figure 4.5 Pressure envelope (minimum and maximum pressures at each computational point, element length 1 m) and pressure profiles at various time instants from the entrance of the transport line up to the location of the first slug.

While the effect of pressure drop as a result of velocity increase is taken into account, the physical movement of the slug is not incorporated. This means that in reality the pressure will drop faster than computed here as more effective space becomes available. Integrating the slug velocity time history (Figure 4.6) over time yields 25 m slug displacement. Consequently, this means a physical gas volume increase of 42%. This volume mismatch does not affect the maximum of the reflected pressure wave, since this maximum occurs in the early stage when the slug has yet to start moving.

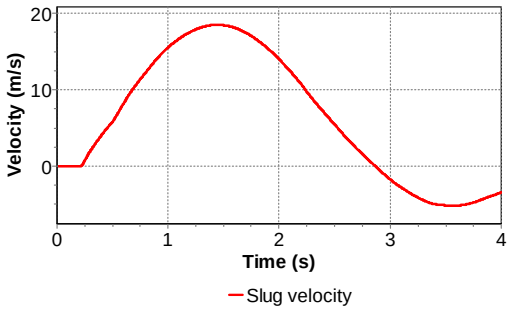

Figure 4.6 Time history of the velocity of the first slug.

Spatial profiles at t = 0.034s of pressure, velocity, temperature and density in between the choke valve and HIPPS valves are shown in Figure 4.7. These profiles illustrate the propagating shock-wave recognized in pressure, velocity, temperature and density. The material wave is recognized in the temperature and density profiles only. While the shock-wave moves at acoustic adiabatic wave speed (Eq. 6), the material wave moves at convective speed (approximately 70 m/s). The displacement of the material wave yields 70·0.034 = 2.4 m

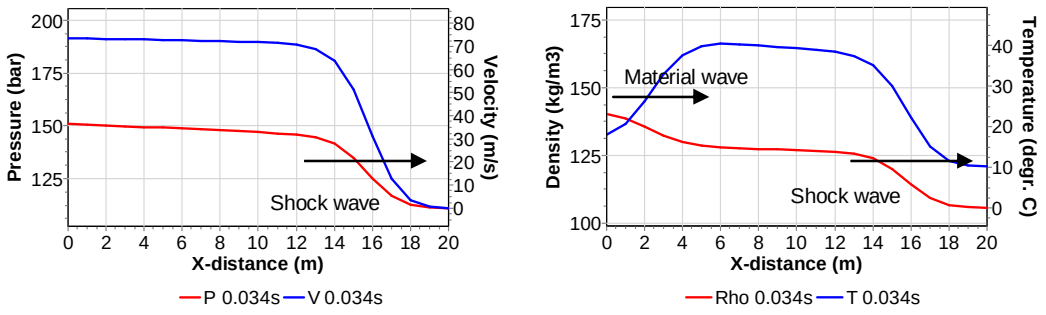

Figure 4.7 Spatial profiles of pressure and velocity (left) and density and temperature (right) from the choke valve up to the HIPPS valves at t = 0.034 s.

5 CONCLUSIONS

In this paper, we have presented a gas model which takes into account the full gas thermodynamics. In this way, the code is able to simulate fast transient phenomena for which the isothermal gas flow assumption does not hold. Furthermore, the code enables for solving gas flow with velocities comparable to the adiabatic pressure wave speed.

The code has been successfully validated against a classical shock-tube benchmark experiment.

The code has been further extended with a slug model based on conservative principles. With this extension, the code allows for solving multi-phase applications encountered in practice. The choke valve break-out scenario is an example of a fast transient multi-phase phenomenon. While direct hydrodynamic interactions between the phases are not considered, the code successfully enables the prediction the pressures in the pipeline as a result of failure of the choke valve and taking into account the presence of liquid slugs.

The results of the choke valve break-out application as presented in this paper have shown that the maximum allowable incidental pressure (MAIP) was not exceeded, even with a liquid slug occupying the complete length of the first depression in the pipe profile. For this particular system, the HIPPS valves react too slowly since the maximum pressure in the transport line was reached within the reaction time of the valves (0.7 seconds). The results provided a detailed insight in the pressure reflections on liquid slugs as a function of slug length (i.e. slug inertia). Furthermore, the presence of a second 'material' wave travelling at the convective gas speed was revealed in the density results near the choke-valve.

The WANDA code has already proven in the past its potential in predicting surge problems in single phase water systems to a high level of accuracy (including cavitation effects, column separation effects and some free surface flow effects). The code has been frequently validated against experimental benchmark data and data of practical applications. This work is an important step to broaden the WANDA suitability by providing a solid foundation to embed the gas model within the WANDA environment. The future direction is towards WANDA multi-phase in which inter-phase hydrodynamic interactions are accounted for as well.

REFERENCES

Huber, P.W., Fitton, C.E.Jr., Delpino, F., *Experimental Investigation of Moving Pressure Disturbances and Shock Waves and Correlation with One-dimensional Unsteady Flow,* NACA Tech. Note, No. 1903, 1949.

Wylie, E.B., Streeter, V.L., *Fluid Transients in Systems,* Prentice Hall, NJ, 1993.